The Astrophysical Journal Letters, 798:L36 (5pp), 2015 January 10 doi:10.1088/2041-8205/798/2/L36

SHORT GAMMA-RAY BURSTS IN THE "TIME-REVERSAL" SCENARIO

Riccardo Ciolfi[1,2] and Daniel M. Siegel[2]
[1] Physics Department, University of Trento, Via Sommarive 14, I-38123 Trento, Italy; riccardo.ciolfi@unitn.it
[2] Max Planck Institute for Gravitational Physics (Albert Einstein Institute), Am Mühlenberg 1, D-14476 Potsdam-Golm, Germany; daniel.siegel@aei.mpg.de
Received 2014 November 11; accepted 2014 December 12; published 2014 December 31

ABSTRACT

Short gamma-ray bursts (SGRBs) are among the most luminous explosions in the universe and their origin still remains uncertain. Observational evidence favors the association with binary neutron star or neutron star–black hole (NS–BH) binary mergers. Leading models relate SGRBs to a relativistic jet launched by the BH-torus system resulting from the merger. However, recent observations have revealed a large fraction of SGRB events accompanied by X-ray afterglows with durations $\sim 10^2$–10^5 s, suggesting continuous energy injection from a long-lived central engine, which is incompatible with the short ($\lesssim$1 s) accretion timescale of a BH-torus system. The formation of a supramassive NS, resisting the collapse on much longer spin-down timescales, can explain these afterglow durations, but leaves serious doubts on whether a relativistic jet can be launched at the merger. Here we present a novel scenario accommodating both aspects, where the SGRB is produced after the collapse of a supramassive NS. Early differential rotation and subsequent spin-down emission generate an optically thick environment around the NS consisting of a photon-pair nebula and an outer shell of baryon-loaded ejecta. While the jet easily drills through this environment, spin-down radiation diffuses outward on much longer timescales and accumulates a delay that allows the SGRB to be observed before (part of) the long-lasting X-ray signal. By analyzing diffusion timescales for a wide range of physical parameters, we find delays that can generally reach $\sim 10^5$ s, compatible with observations. The success of this fundamental test makes this "time-reversal" scenario an attractive alternative to current SGRB models.

Key words: black hole physics – gamma-ray burst: general – magnetohydrodynamics (MHD) – stars: magnetic field – stars: neutron – X-rays: general

1. INTRODUCTION

Merging binary neutron stars (BNSs) and neutron star–black hole (NS–BH) systems represent the leading scenarios to explain the phenomenology of short gamma-ray bursts (SGRBs; e.g., Paczynski 1986; Eichler et al. 1989; Narayan et al. 1992; Barthelmy et al. 2005; Fox et al. 2005; Gehrels et al. 2005; Shibata et al. 2006; Rezzolla et al. 2011; Paschalidis et al. 2014; Tanvir et al. 2013) and are among the most promising sources of gravitational waves (GWs) for the detection with interferometric detectors such as advanced LIGO and Virgo (Harry et al. 2010; Accadia et al. 2011). It is generally assumed that within $\lesssim$100 ms after the merger, a BH-torus system forms that can power a transient relativistic jet through accretion and thus produce the SGRB emission lasting $\lesssim$2 s (e.g., Shibata et al. 2006; Rezzolla et al. 2011; Paschalidis et al. 2014).

Recent observations by the *Swift* satellite (Gehrels et al. 2004) have revealed long-lasting, "plateau-shaped" X-ray afterglows in the vast majority of observed SGRB events (e.g., Rowlinson et al. 2013; Gompertz et al. 2014). These afterglows indicate ongoing energy injection by a central engine on timescales up to $\sim 10^4$ s, which is commonly interpreted as magnetic spin-down radiation from an (in)definitely stable NS formed in a BNS merger (referred to as the "magnetar model"; Metzger et al. 2008; Zhang & Mészáros 2001).

While recent observations of high-mass neutron stars (Demorest et al. 2010; Antoniadis et al. 2013) indicate a rather stiff equation of state and make the formation of a long-lived or even stable NS a likely possibility in the majority of BNS merger events, the existence of long-lasting, sustained X-ray afterglows challenge, in particular, the NS–BH progenitor scenario, as a NS cannot be formed in this case. More severe, however, is the following apparent dichotomy. On the one hand, a BH-torus system with accretion timescales of less than one second cannot sustain continuous energy emission on timescales $\lesssim 10^4$ s. On the other hand, while the magnetar model can explain the long-lasting X-ray afterglows, it cannot readily explain how the prompt SGRB should be generated. Despite attempts to explain the prompt emission in a way that is similar to long gamma-ray bursts (Bucciantini et al. 2012), numerical simulations of BNS mergers have not found indications for the formation of a jet when a remnant NS is formed (e.g., Giacomazzo & Perna 2013).

Here we propose a new scenario that can solve this dichotomy. This scenario assumes a BNS merger that produces a long-lived NS, which emits spin-down radiation and eventually collapses to a BH-torus system. While the relativistic jet produced by the BH-torus system can easily drill through, the spin-down emission is trapped in a photon-pair plasma nebula and an outer shell of matter ejected shortly after the NS is formed. The resulting delay can effectively reverse the observation times of the two signals and can explain why the X-ray emission powered by the NS spin-down is (in part) observed after the prompt SGRB emission.

The idea that a delayed afterglow emission could solve the problem has also been proposed in a parallel work by Rezzolla & Kumar (2014), although with a different phenomenology.[3] In this Letter, we focus on showing that the time delay between the prompt SGRB and the long-lasting X-ray signal can be large enough to explain the observed X-ray afterglow durations. This represents a fundamental validation (not considered by

[3] This idea was originally discussed during the preparation of Siegel et al. (2014) among the three authors, but since then it has been independently developed in divergent ways.

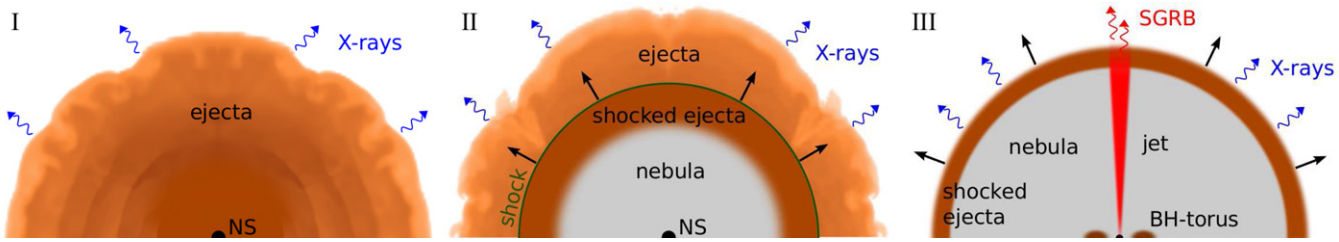

Figure 1. Evolution phases: (I) the differentially rotating supramassive NS ejects a baryon-loaded and highly isotropic wind; (II) the cooled-down and uniformly rotating NS emits spin-down radiation inflating a photon-pair nebula that drives a shock through the ejecta; (III) the NS collapses to a BH, a relativistic jet drills through the nebula, and the ejecta shell and produces the prompt SGRB, while spin-down emission diffuses outward on a much longer timescale.

Rezzolla & Kumar 2014) and a necessary condition to make the scenario worth considering.

2. PHENOMENOLOGY

The merger of two NSs forms a differentially rotating object. The time-reversal scenario proposed here requires that the merger remnant is a supramassive NS, i.e., a NS with mass above the maximum mass for nonrotating configurations $M_{\rm TOV}$, but below the maximum mass for uniformly rotating configurations $M_{\rm max}$, where $M_{\rm max} \approx 1.15$–$1.20\,M_{\rm TOV}$ (Lasota et al. 1996).[4] This implies that the NS does not require differential rotation to support it against gravitational collapse, and the latter is prevented by uniform rotation as long as the spin rate is high enough; therefore, the time of collapse to a BH is typically of the order of the spin-down timescale. Given that the mass distribution of BNSs peaks around 1.3–$1.4\,M_\odot$ (Belczynski et al. 2008) and that recent observations find NS masses as large as $\simeq 2\,M_\odot$ (Demorest et al. 2010; Antoniadis et al. 2013), supramassive NS merger remnants are a very likely possibility.

In addition to mass ejection associated with the merger process, the newly born NS can launch baryon-loaded winds (see Figure 1, (I)), either produced by large magnetic pressure gradients at the stellar surface due to magnetic field amplification in the differentially rotating stellar interior (Siegel et al. 2013, 2014; Kiuchi et al. 2014), or induced by neutrino emission (e.g., Dessart et al. 2009). Both mechanisms can typically produce mass-loss rates of $\dot{M} \sim 10^{-3}\,M_\odot\,{\rm s}^{-1}$ (Dessart et al. 2009; Siegel et al. 2014). While baryon pollution resulting from dynamical merger ejecta (e.g., Hotokezaka et al. 2013; Rosswog et al. 2013) is mostly restricted to the orbital plane, the magnetically and neutrino-induced winds are highly isotropic, with bulk speeds $\sim 0.1c$ (Siegel et al. 2014). Magnetically induced winds are associated with differential rotation, which can only last for at most $t_{\rm dr} \sim 0.1$–10 s, assuming typical initial magnetic field strengths $B \sim 10^{13}$–10^{15} G (Shapiro 2000; Siegel et al. 2014). Note that during this timescale the initial magnetic fields can be amplified by orders of magnitude. For neutrino-induced winds, the typical cooling timescales are $\lesssim 1$ s (Dessart et al. 2009); therefore, they can also last no longer than $\sim t_{\rm dr}$.

At $t \sim t_{\rm dr}$, the merger remnant has settled down to a uniformly rotating, strongly magnetized NS and further mass ejection is suppressed. As the baryon density in the surrounding of the NS drops, the NS starts to emit electromagnetic (EM) spin-down radiation at the expense of rotational energy, with luminosity $L_{\rm sd} = L_{\rm sd}^{\rm in}\,(1 + t/t_{\rm sd})^{-2}$, where

$$L_{\rm sd}^{\rm in} \simeq 1.5 \times 10^{49}\,B_{\rm p,15}^2\,R_6^3\,P_{\rm in,-3}^{-4}\ {\rm erg\ s^{-1}}. \quad (1)$$

[4] The NS could also be hypermassive, i.e., with mass above $M_{\rm max}$, if it migrates below this limit by substantial mass loss before differential rotation is removed.

Here, $B_{\rm p}$ and $P_{\rm in}$ are the surface magnetic field strength and initial spin period at $t \sim t_{\rm dr}$, respectively, R is the NS radius, and

$$t_{\rm sd} \simeq 2.7 \times 10^3\,B_{\rm p,15}^{-2}\,R_6^{-3}\,P_{\rm in,-3}^2\ {\rm s} \quad (2)$$

is the spin-down timescale.

The spin-down emission inflates a photon-pair plasma nebula (henceforth "nebula"; Lightman & Zdziarski 1987) behind the expanding ejecta (see Figure 1, (II)). The high photon pressure associated with this photon-pair plasma drives a strong shock through the ejecta, which sweeps up the material into a thin shell while rapidly propagating toward the outer ejecta radius. At shock breakout, a transient signal observed as an early precursor to the SGRB (Troja et al. 2010) could be produced. Nebula energy is deposited in the optically thick ejecta and converted into thermal and kinetic energy, causing a rapid acceleration of the ejecta to relativistic speeds $v_{\rm ej} \lesssim 0.8$–$0.9c$ (Metzger & Piro 2014).

The injection of spin-down energy into the nebula ceases at $t = t_{\rm coll}$, when rotation can no longer prevent the NS from collapsing to a BH. Within millisecond timescales, a BH-torus system forms and generates the necessary conditions to launch a relativistic jet of duration $\lesssim 0.01$–1 s, which corresponds to the typical accretion time of the torus (e.g., Narayan et al. 1992; Shibata et al. 2006; Rezzolla et al. 2011). This jet drills through the ejecta shell and eventually breaks out, producing the prompt SGRB emission (see Figure 1, (III)).

As the nebula and the ejecta shell are optically thick for the times of interest, the spin-down energy radiated away by the NS up to $t_{\rm coll}$ emerges from the outer radius of the ejecta shell with a substantial delay, producing the observed long-lasting X-ray afterglow radiation. Compared to this delay, the timescale for the jet to drill through the ejecta and to break out is orders of magnitudes smaller (see Section 3). Hence, the spin-down emission, although produced before the jet is formed, can be observed for a long time after the prompt gamma-ray emission.

An important point to stress is that in the time-reversal scenario the observed X-ray afterglow durations correspond to such a delay and not to the spin-down timescale of the NS.

3. TIMING ARGUMENT

The crucial validation to assess whether the time-reversal scenario outlined above can be compatible with the combined observations of SGRB prompt emission and long-lasting X-ray afterglows comes from the analysis of the photon diffusion timescales associated with the nebula and the ejecta. The scenario cannot hold unless the delay of the signal produced by the NS spin-down just before the collapse can account for the observed duration of the X-ray afterglow.

The argument proceeds as follows. From observations (e.g., Rowlinson et al. 2013), we can assume that the NS exists

for a time $t_{\rm coll} \gtrsim t_{\rm sd}$. Furthermore, we typically have $t_{\rm sd} \gg t_{\rm dr} + \Delta t_{\rm shock} \equiv t_{\rm shock,out}$, where $\Delta t_{\rm shock}$ is the time needed by the shock to propagate outward through the ejecta. Consequently, at $t_{\rm coll}$ the ejecta has already been compressed into a thin shell of thickness $\Delta_{\rm ej}$, which moves outward at relativistic speeds.

Most of the emission from the NS cannot reach the outer radius $R_{\rm ej}$ of the ejecta shell later than $t_{\rm NS,out} = t_{\rm coll} + \Delta t_{\rm NS,out}$, where $\Delta t_{\rm NS,out}$ is the total time of photon diffusion across the nebula and the ejecta shell. At $t_{\rm NS,out}$, any photon that was present in the system at $t_{\rm coll}$ has had enough time to escape; therefore, the emission is suppressed for $t \gtrsim t_{\rm NS,out}$. The corresponding delay with respect to the light travel time is given by $t_{\rm NS}^{\rm delay} = \Delta t_{\rm NS,out} - R_{\rm ej}(t_{\rm NS,out})/c$.

The emission from the jet is also delayed due to the time to launch the jet after the collapse (∼ms) and the fact that the jet has to propagate outward through the nebula and the ejecta shell with an effective speed smaller than c. While the propagation speed through the baryon-poor nebula is very close to c, the drill time through the ejecta shell dominates the total delay $t_{\rm jet}^{\rm delay}$.

Assuming a non-relativistic jet head speed, the drill time across the ejecta can be estimated by (Bromberg et al. 2011)

$$t_{\rm drill} \simeq 2.5 \times 10^{-4} \Delta_{\rm ej,9}^{5/3} \rho_{\rm ej,-7}^{1/3} (\theta_{\rm jet}/30^\circ)^{1/3} L_{\rm jet,47}^{-1/3} \ {\rm s}, \quad (3)$$

where $\rho_{\rm ej}$ denotes the density of the ejecta shell, $\theta_{\rm jet}$ the jet opening angle, and $L_{\rm jet}$ the jet luminosity. For typical parameter values, however, Equation (3) yields a drill time smaller than the corresponding light travel time, which indicates that the jet head speed has to be relativistic. This is mainly due to the very low densities at $t \gtrsim t_{\rm coll}$ (see Section 4). Consequently, $t_{\rm jet}^{\rm delay}$ is negligible with respect to the other timescales of interest.

In conclusion, a necessary condition to explain a certain duration of the X-ray afterglow, $\Delta t_{\rm afterglow}$, is given by

$$t_{\rm NS}^{\rm delay} \simeq t_{\rm NS}^{\rm delay} - t_{\rm jet}^{\rm delay} \gtrsim \Delta t_{\rm afterglow}. \quad (4)$$

4. COMPUTATION OF DIFFUSION TIMESCALES

We compute the diffusion timescales and, hence, $t_{\rm NS}^{\rm delay}$ in terms of the following parameters: the timescale for removal of differential rotation $t_{\rm dr}$, the mass ejection rate $\dot{M}$ (as long as differential rotation is sustained, i.e., for $t < t_{\rm dr}$), the magnetic field strength at the pole, $B_{\rm p}$, and the initial rotation period $P_{\rm in}$ of the NS once it has settled down to uniform rotation. Moreover, we need to specify the time $t_{\rm shock,out}$ at which the shock reaches the outer ejecta radius $R_{\rm ej}$, the expansion speed of the ejecta before and after $t_{\rm shock,out}$, $v_{\rm ej}^0$ and $v_{\rm ej}$, respectively, the pair yield in the nebula, Y, and the ejecta opacity κ. For the last two parameters, we assume canonical values $Y \sim 0.1$ and $\kappa \sim 0.2$ cm^2 g^{-1} (Metzger & Piro 2014).

At $t = t_{\rm dr}$, the NS is still surrounded by a baryon-loaded and nearly isotropic wind that extends up to $R_{\rm ej}(t_{\rm dr}) = v_{\rm ej}^0 t_{\rm dr}$ and has an average density of $\rho_{\rm ej}(t_{\rm dr}) = 3 t_{\rm dr} \dot{M}/[4\pi R_{\rm ej}^3(t_{\rm dr})]$. Once differential rotation is removed, mass ejection is suppressed and spin-down emission drives a strong shock through the ejecta that rapidly ($t_{\rm shock,out} \sim t_{\rm dr}$) sweeps up the ejecta mass ($M_{\rm ej} \simeq t_{\rm dr}\dot{M}$) into a thin shell of shocked fluid with thickness $\Delta_{\rm ej}$. From the Rankine-Hugoniot conditions for a strong shock and assuming an ideal fluid equation of state for the ejecta with $\Gamma = 4/3$, shock compression produces a jump in density of a factor of 7, i.e., at $t = t_{\rm shock,out}$:

$$\rho_{\rm ej} = \frac{M_{\rm ej}}{4\pi R_{\rm ej}^2 \Delta_{\rm ej}} = \frac{21}{4\pi} \frac{\dot{M} t_{\rm dr}}{R_{\rm so}^3}, \quad (5)$$

where $R_{\rm so} \equiv R_{\rm ej}(t_{\rm shock,out})$. This allows us to compute the corresponding shell thickness $\Delta_{\rm ej} = R_{\rm so}/21$, which we assume to be constant for $t > t_{\rm shock,out}$. After $t_{\rm shock,out}$, the ejecta shell is rapidly accelerated to its asymptotic speed $v_{\rm ej}$. The density of the shell for $t \gg t_{\rm shock,out}$ is thus given by

$$\rho_{\rm ej}(t) = \frac{21}{4\pi} \frac{\dot{M} t_{\rm dr}}{R_{\rm so}[R_{\rm so} + v_{\rm ej}(t - t_{\rm shock,out})]^2}. \quad (6)$$

If the ejecta shell at time $t \gg t_{\rm shock,out}$ was at rest, the associated "static" photon diffusion timescale would be

$$t_{\rm diff}^{\rm ej,stat}(t) = \frac{\Delta_{\rm ej}}{c}(1 + \kappa \rho_{\rm ej}(t) \Delta_{\rm ej}), \quad (7)$$

where we have added the light travel time to account for a possible transition to the optically thin regime. Similarly, if the nebula was not expanding, the associated diffusion timescale resulting from the electron–positron pairs would be given by (Lightman & Zdziarski 1987)

$$t_{\rm diff}^{\rm n,stat}(t) = \frac{R_{\rm n}(t)}{c} \left(1 + \sqrt{\frac{4 Y \sigma_{\rm T} L_{\rm sd}(t)}{\pi R_{\rm n}(t) m_{\rm e} c^3}} \right), \quad (8)$$

where $\sigma_{\rm T}$ denotes the Thomson cross section, $m_{\rm e}$ the electron mass, $L_{\rm sd}$ the spin down luminosity, and $R_{\rm n}(t) \equiv R_{\rm ej}(t) - \Delta_{\rm ej}$ the radius of the nebula. Note that for $t > t_{\rm sd}$, both $t_{\rm diff}^{\rm ej,stat}$ and $t_{\rm diff}^{\rm n,stat}$ are monotonically decreasing functions of time.

The actual photon diffusion timescales differ from Equations (7) and (8), as the properties of the system (e.g., $R_{\rm ej}$ and $\rho_{\rm ej}$) can significantly change while a photon is propagating outward. Nevertheless, Equations (7) and (8) can be employed to derive lower and upper bounds. For a photon emitted by the NS just before $t_{\rm coll}$, an upper bound on the total diffusion time through the nebula and the ejecta is given by the sum of the two static diffusion times at $t_{\rm coll}$ (thanks to the monotonicity property mentioned above): $t_{\rm diff} \lesssim t_{\rm diff}^{\rm ej,stat}(t_{\rm coll}) + t_{\rm diff}^{\rm n,stat}(t_{\rm coll})$. Hence,

$$t_{\rm NS}^{\rm delay} \lesssim t_{\rm diff}^{\rm ej,stat}(t_{\rm coll}) + t_{\rm diff}^{\rm n,stat}(t_{\rm coll}) - R_{\rm ej}(t_{\rm coll})/c. \quad (9)$$

A lower bound on $t_{\rm NS}^{\rm delay}$ can be placed by

$$t_{\rm NS}^{\rm delay} \gtrsim t_{\rm diff}^{\rm ej,stat}(t_{\rm coll}^*) + t_{\rm diff}^{\rm n,stat}(t_{\rm coll}^*) - R_{\rm ej}(t_{\rm coll}^*)/c, \quad (10)$$

where $t_{\rm coll}^*$ is given by $t_{\rm coll}^* = t_{\rm coll} + t_{\rm diff}^{\rm ej,stat}(t_{\rm coll}^*) + t_{\rm diff}^{\rm n,stat}(t_{\rm coll}^*)$. As a conservative estimate of $t_{\rm NS}^{\rm delay}$ to be used in checking the validity of Equation (4), we henceforth use the lower limit given by Equation (10).

Figures 2 and 3 summarize results for $t_{\rm NS}^{\rm delay}$ over the entire parameter space. Reliable estimates can only be provided as long as the ejecta shell is still optically thick at $t_{\rm coll}^*$ and thus confines the nebula. Figure 2 shows $t_{\rm NS}^{\rm delay}$ for a range of $t_{\rm dr}$, $B_{\rm p}$, and $P_{\rm in}$. The optical depths decrease for decreasing values of $B_{\rm p}$ and increasing values of $P_{\rm in}$, as the spin-down timescale and thus $t_{\rm coll}$ increase (see Equation (2)). In particular, the ejecta has more time to expand and thus becomes optically

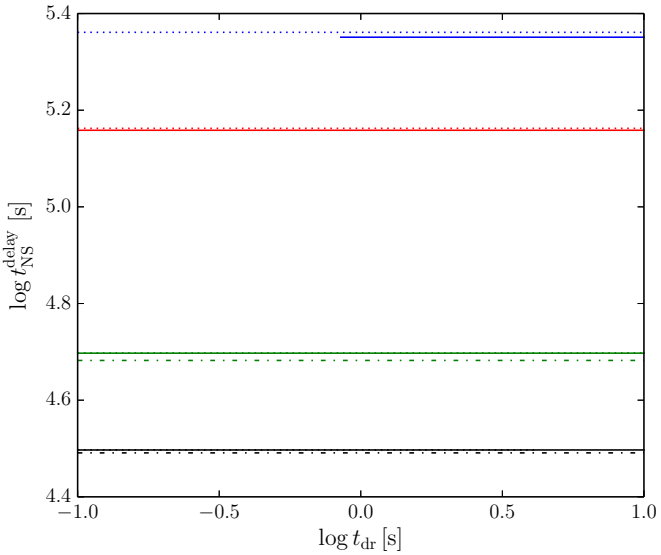

Figure 2. Estimated delay for a photon emitted just before collapse as a function of $t_{\rm dr}$, for $B_{\rm p} = 5\times10^{14}$, 10^{15}, 5×10^{15}, 10^{16} G (from top to bottom) and $P_{\rm in} = 0.5$, 1, 5 ms (dotted, solid, dash-dotted), assuming $v_{\rm ej}^0 = 0.1c$, $v_{\rm ej} = 0.5c$, $\dot{M} = 10^{-3}\ M_\odot\ {\rm s}^{-1}$, $t_{\rm coll} = t_{\rm sd}$. Shown are only cases in which the ejecta shell is still optically thick.

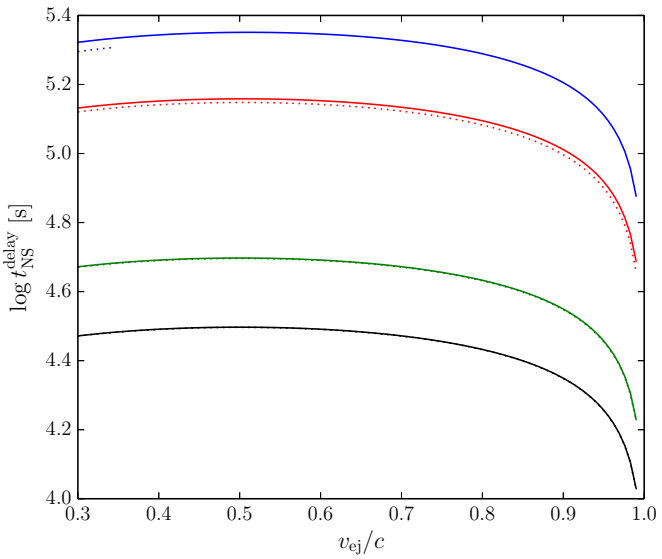

Figure 3. Estimated delay for a photon emitted just before collapse as a function of the shell expansion speed $v_{\rm ej}$, for $B_{\rm p} = 5\times10^{14}$, 10^{15}, 5×10^{15}, 10^{16} G (from top to bottom) and $t_{\rm coll} = t_{\rm sd}$ (solid), $t_{\rm coll} = 5t_{\rm sd}$ (dotted), assuming $v_{\rm ej}^0 = 0.1c$, $t_{\rm dr} = 10$ s, $\dot{M} = 10^{-3}\ M_\odot\ {\rm s}^{-1}$, $P_{\rm in} = 1$ ms. Shown are only cases in which the ejecta shell is still optically thick.

thinner. The results are not shown for the cases in which the ejecta shell is optically thin. As long as the ejecta are optically thick, $t_{\rm NS}^{\rm delay}$ is insensitive to the value of $t_{\rm dr}$ in the range ∼0.1–10 s. We have further verified that the same holds for expected mass-loss rates $\dot{M} \sim 10^{-4}$–$10^{-2}\ M_\odot\ {\rm s}^{-1}$, shock propagation times $\Delta t_{\rm shock} \sim 0$–$100 t_{\rm dr}$, and initial wind speeds $v_{\rm ej}^0 \sim 0.01$–$0.1c$. This is because the diffusion time of the nebula is much larger than the diffusion time of the ejecta shell for the times of interest. Hence, $t_{\rm NS}^{\rm delay}$ is largely insensitive to the properties of the shell.

Figure 3 reports results on $t_{\rm NS}^{\rm delay}$ as a function of the two most influential parameters of our model, the magnetic field strength of the NS, $B_{\rm p}$, and the asymptotic ejecta shell velocity $v_{\rm ej}$. For $B_{\rm p} \gtrsim 5\times10^{14}$ G, the ejecta shell is still optically thick at $t_{\rm coll}^*$ for $t_{\rm coll} \approx t_{\rm sd}$ (solid lines). The dotted curves indicate that for $t_{\rm coll}/t_{\rm sd} \gtrsim 5$ and low magnetic field strengths the ejecta matter can become optically thin. Figure 3 also shows that the results only become sensitive to $v_{\rm ej}$ for highly relativistic speeds.

From our estimates, we conclude that in the parameter ranges $B_{\rm p} \sim 10^{14}$–10^{16} G, $P_{\rm in} \sim 0.5$–5 ms, $t_{\rm dr} \sim 0.1$–10 s, $\dot{M} \sim 10^{-4}$–$10^{-2}\ M_\odot\ {\rm s}^{-1}$, $v_{\rm ej}^0 \sim 0.01$–$0.1c$, the delay times $t_{\rm NS}^{\rm delay}$ are larger than 3×10^4 s and larger than $\sim10^5$ s for $B_{\rm p} \lesssim 10^{15}$ G. Therefore, according to our criterion given in Equation (4), the observed durations of X-ray afterglows of $\Delta t_{\rm afterglow} \sim 10^2$–$10^5$ s (e.g., Rowlinson et al. 2013; Gompertz et al. 2014) are compatible with the proposed time-reversal scenario.

5. DISCUSSION

In our scenario, the long-lasting (∼10^2–10^5 s) X-ray afterglow emission accompanying a large fraction of SGRBs is produced by a long-lived supramassive NS, which eventually collapses to a BH on the spin-down timescale and thus generates the necessary conditions for a relativistic jet to be launched. While the jet can easily drill through the surrounding photon-pair plasma and baryon-loaded ejecta, spin-down radiation emitted by the NS before the collapse diffuses outward on a much longer timescale, accumulating a significant delay before finally escaping. This delay explains how the X-ray emission powered by spin-down radiation before the collapse is observed in part before and in part after the prompt emission. The optically thick nebula and ejecta are therefore responsible for a "time reversal" of the observed signals.

In our simple analysis, we have focused on the estimation of the maximum delay that can affect the spin-down radiation, depending on the most relevant properties of the system. If this delay is shorter than the duration of an observed X-ray afterglow, the latter cannot be explained within the time-reversal scenario. Therefore, this test is crucial to make the scenario worth considering.

By exploring a wide range of physical parameters, we find that in most cases, afterglow durations of up to 10^4–10^5 s are compatible with the estimated delays. Moreover, we find that the maximum delay is always determined by the high optical depth of the nebula, which dominates over the optical depth of the ejecta.

One important consequence of this new scenario is that for all SGRB events accompanied by a long-lasting X-ray afterglow, the progenitor would be necessarily a BNS and not a BH-NS binary. Furthermore, the peak amplitude of GW emission associated with the time of the merger would reach the observer long before the EM prompt SGRB signal. The two signals would be separated by the lifetime of the supramassive NS, which can easily exceed $\sim10^3$ s, with profound consequences for coincident GW and EM observations. This separation would provide an accurate measurement of the NS lifetime (to better than 1%).

A supporting piece of evidence for our scenario comes from the observation of steep decay phases in some of the X-ray afterglow light curves, which are interpreted as a collapse to a BH (e.g., Rowlinson et al. 2013). These features are in favor of the long-lived supramassive NS assumed here. A strong indication for the time-reversal scenario would come from the observation of X-ray "afterglow" emission prior to the SGRB itself, i.e., of a plateau-like X-ray light curve with the prompt emission in between. This would be indicative of

a change in arrival times with respect to the emission times of the two signals. Moreover, the observation of "orphan" SGRB-like events, with a plateau-like X-ray emission, but missing prompt emission, can confirm the isotropy of the afterglow radiation we expect. In this case, the collimated prompt emission would be beamed away from us.

A potential difficulty is posed by the observation of several SGRB events in which the X-ray afterglow light curve shows a late-time decay compatible with $L_X \propto t^{-2}$. This is the behavior expected for spin-down radiation at $t > t_{sd}$ (see above Equation (1)). In our scenario, we need to explain how this particular decay is not altered by the optically thick environment surrounding the NS. We find that for the cases considered here, the delay due to the diffusion time of photons through the ejecta shell at times $t \gtrsim t_{sd}$ is typically orders of magnitude smaller than the spin-down timescale and, thus, such diffusion should have no effect on the time behavior of the signal luminosity. The diffusion timescale associated with the nebula, however, is not smaller than the spin-down timescale and whether the trapped radiation would still emerge with the same time dependence as the spin-down injection luminosity remains in doubt.

We thank B. Schutz and W. Kastaun for valuable discussions. R.C. acknowledges support from MIUR FIR grant No. RBFR13QJYF.

REFERENCES

Accadia, T., Acernese, F., Antonucci, F., et al. 2011, CQGra, 28, 114002
Antoniadis, J., Freire, P. C. C., Wex, N., et al. 2013, Sci, 340, 448
Barthelmy, S. D., Chincarini, G., Burrows, D. N., et al. 2005, Natur, 438, 994
Belczynski, K., O'Shaughnessy, R., Kalogera, V., et al. 2008, ApJL, 680, L129
Bromberg, O., Nakar, E., Piran, T., & Sari, R. 2011, ApJ, 740, 100
Bucciantini, N., Metzger, B. D., Thompson, T. A., & Quataert, E. 2012, MNRAS, 419, 1537
Demorest, P. B., Pennucci, T., Ransom, S. M., Roberts, M. S. E., & Hessels, J. W. T. 2010, Natur, 467, 1081
Dessart, L., Ott, C. D., Burrows, A., Rosswog, S., & Livne, E. 2009, ApJ, 690, 1681
Eichler, D., Livio, M., Piran, T., & Schramm, D. N. 1989, Natur, 340, 126
Fox, D. B., Frail, D. A., Price, P. A., et al. 2005, Natur, 437, 845
Gehrels, N., Chincarini, G., Giommi, P., et al. 2004, ApJ, 611, 1005
Gehrels, N., Sarazin, C. L., O'Brien, P. T., et al. 2005, Natur, 437, 851
Giacomazzo, B., & Perna, R. 2013, ApJ, 771, L26
Gompertz, B. P., O'Brien, P. T., & Wynn, G. A. 2014, MNRAS, 438, 240
Harry, G. M. LIGO Scientific Collaboration 2010, CQGra, 27, 084006
Hotokezaka, K., Kiuchi, K., Kyutoku, K., et al. 2013, PhRvD, 87, 024001
Kiuchi, K., Kyutoku, K., Sekiguchi, Y., Shibata, M., & Wada, T. 2014, PhRvD, 90, 041502
Lasota, J.-P., Haensel, P., & Abramowicz, M. A. 1996, ApJ, 456, 300
Lightman, A. P., & Zdziarski, A. A. 1987, ApJ, 319, 643
Metzger, B. D., & Piro, A. L. 2014, MNRAS, 439, 3916
Metzger, B. D., Quataert, E., & Thompson, T. A. 2008, MNRAS, 385, 1455
Narayan, R., Paczynski, B., & Piran, T. 1992, ApJL, 395, L83
Paczynski, B. 1986, ApJL, 308, L43
Paschalidis, V., Ruiz, M., & Shapiro, S. L. 2014, arXiv:1410.7392
Rezzolla, L., Giacomazzo, B., Baiotti, L., et al. 2011, ApJL, 732, L6
Rezzolla, L., & Kumar, P. 2014, arXiv:1410.8560
Rosswog, S., Piran, T., & Nakar, E. 2013, MNRAS, 430, 2585
Rowlinson, A., O'Brien, P. T., Metzger, B. D., Tanvir, N. R., & Levan, A. J. 2013, MNRAS, 430, 1061
Shapiro, S. L. 2000, ApJ, 544, 397
Shibata, M., Duez, M. D., Liu, Y. T., Shapiro, S. L., & Stephens, B. C. 2006, PhRvL, 96, 031102
Siegel, D. M., Ciolfi, R., Harte, A. I., & Rezzolla, L. 2013, PhRvD, 87, 121302
Siegel, D. M., Ciolfi, R., & Rezzolla, L. 2014, ApJL, 785, L6
Tanvir, N. R., Levan, A. J., Fruchter, A. S., et al. 2013, Natur, 500, 547
Troja, E., Rosswog, S., & Gehrels, N. 2010, ApJ, 723, 1711
Zhang, B., & Mészáros, P. 2001, ApJL, 552, L35